Consideration of dynamic loads in determination of axle load spectra for pavement design

Dawid Rys[a]*

[a] *Faculty of Civil and Environmental Engineering, Gdansk University of Technology, Gdansk, Poland;*

dawid.rys@pg.edu.pl *corresponding author

Consideration of dynamic loads in determination of axle load spectra for pavement design

Axle load spectra constitute a crucial part of the data for pavement design and pavement distress analysis. Typically, axle load spectra represent static load from vehicles and do not include dynamic loads generated by vehicles in motion. While dynamic loads can significantly contribute to faster pavement distress but this fact is mostly omitted in pavement design methods. The paper presents a methodology of consideration of dynamic loads in axle load spectra for mechanistic-empirical pavement design. Calculations of dynamic axle load spectra for pavements of various evenness (expressed by IRI) and various vehicle speeds were performed and discussed. The effect of dynamic axle load spectra on pavement performance was analysed. M-EPDG calculations performed for 3 selected flexible pavements shows that dynamic loads have a minor effect on pavement performance if the pavement is smooth and IRI is close to 1.0 mm/m. The detrimental effects of dynamic axle loads increase rapidly with the pavement evenness deterioration, resulting in faster (up to 25%) development of pavement distresses for IRI = 4.0 mm/m and vehicle speed of 60 km/h. Analysis proved that thinner pavement structures are more sensitive to dynamic loads than thicker structures. The investigation of vehicle speed impact on vehicle dynamic loads and pavement performance showed that at low vehicle speed (30 km/h) dynamic loads have a minor effect and pavement distress results mostly from a decrease in stiffness modulus of asphalt mixture and increase in permanent deformations, while for vehicle speeds higher than 90 km/h dynamic loads significantly contribute to pavement distress and adverse dynamic effects are not compensated by an increase in stiffness modulus of asphalt mixtures. The results also emphasize the significance of proper pavement evenness maintenance, especially on high speed motorways.

Keywords: flexible pavements, pavement design, M-EPDG, axle load spectra, traffic loading, vehicle, dynamic loads, axle load, distribution of axle loads, Weigh in Motion, traffic input data

Introduction

Background

The dynamics of vehicle movement are directly related to pavement evenness. Due to roughness of pavement, loads from moving vehicle axles vary from static loads. The distribution of dynamic loads is similar to normal distribution and can be described by the static load, which corresponds to their mean value, and the Dynamic Load Coefficient (DLC), which corresponds to coefficient of variation. With the deterioration of pavement evenness and the increase in the roughness index IRI, the coefficient DLC increases and the detrimental effect of axle load on pavement structure increases as well. New pavements, especially on motorways, have good quality in terms of evenness, during the service, however, their quality deteriorates. Moreover, according to the study of (Can et al., 2016) some technologies of repairs and rehabilitation of old pavements do not ensure satisfactory initial pavement evenness or result in fast progress of evenness deterioration. (Davis, 2010) reported that neither roughness values nor peak wheel forces are included in Australian pavement design models. This statement can be broadened to encompass many common design methods, including AASHTO 1993, catalogues of typical pavement structures used in several European Union countries as well as the Mechanistic-Empirical Pavement Design Guide (M-EPDG). Traffic load in pavement design is described by axle load spectra, which are used to determine Load Equivalency Factors or Truck Factors, or pose a significant part of input data, in the case of the M-EPDG. However, axle load spectra are determined on the basis of static loads and do not consider dynamic effects of vehicles.

Objective

The objective of this article is to assess the impact of heavy vehicle dynamic loading resulting from pavement roughness and vehicle speed on axle load spectra. Furthermore, the effect of consideration of dynamic loads in axle load spectra on the calculated pavement deterioration process is investigated. To this purpose, analyses of three example flexible pavements loaded with static and dynamic axle load spectra have been performed in accordance with the M-EPDG.

Literature review

Vehicle dynamic loads

The dynamic tyre forces generated by vehicles are typically observed to be close to normal distribution. According to research carried out by (Gillespie et al., 1992), for such probability distributions the expected value is usually equal to the static load value. The parameter known as Dynamic Load Coefficient (DLC) is frequently used to characterize the magnitude of dynamic tyre forces and it is defined as:

$$DLC = \frac{\sigma}{\bar{F}} \tag{1}$$

where:

σ – standard deviation of axle loading force, $\bar{F}$ – mean value of axle loading force, approximately equal to static loading.

In order to estimate the DLC parameter, several researchers measured in situ the dynamic loads generated by vehicle wheels, using sensors installed in the vehicles (Cebon, 1999; Cole, D. J., 1989; Davis, 2010; Davis & Bunker, 2011; Moran & Sullivan, 1995; Sweatman, 1983). According to the report given by Cebon (1999) the DLC delivered from in-situ measurement ranges from 0.05 to 0.4. Potentially, the DLC parameter can be obtained from measurements delivered from sensors mounted on tyre-

pavement interface, like multi-sensor Weigh in Motion (Piotr Burnos et al., 2007; Gajda, Burnos, & Sroka, 2018) or Stress in Motion measuring mat (De Beer & Fisher, 2013). Other researchers used mathematical models of truck suspension and measured road profile to simulate the dynamic tyre forces and to calculate the DLC parameter (Buhari, Md Rohani, & Abdullah, 2013; Misaghi, Nazarian, & C. J. Carrasco, 2010; Sun, 2013). The simulations carried out by (Cole & Cebon, 1992; Imine, Delanne, & M'Sirdi, 2006; Park, Papagiannakis, & Kim, 2014; Shi & Cai, 2009) replaced the model of one wheel and its suspension with a model of the whole vehicle. The results of these studies imply that DLC increases with vehicle speed and deterioration of pavement evenness. Suspension type, its stiffness and damping coefficient has major effect on DLC, while the vehicle body (sprung mass) has minor effect. In the further parts of these studies the effect of variation in suspension parameters on dynamic forces is not considered and analyses are focused on the effect of vehicle speed and pavement roughness. A summary of relationships between vehicle speed, pavement roughness and DLC was prepared on the basis of literature review and it is given in Table 1.

As shown in Table 1, the DLC parameter is related to the International Roughness Index (IRI). IRI was developed by the World Bank in the 1980s. Because IRI reflects ride quality and comfort level of road users it was adopted by road authorities in many territories as a pavement performance indicator. In spite of numerous other available approaches to quantify the longitudinal road roughness, IRI seems to be the most popular (Peter Múčka, 2017a). Due to the importance of IRI, many research efforts were devoted to IRI modelling and predictions (Abdelaziz, Abd El-Hakim, El-Badawy, & Afify, 2018; Amarendra Kumar & Ashoke Kumar, 2013; Perera, Byrum, & Kohn, 1998; Sylvestre, Bilodeau, & Doré, 2017; Ziari, Sobhani, Ayoubinejad, & Hartmann, 2015).

Newly constructed pavements have average IRI in the range from 0.9 to 1.2, but locally the maximum IRI can exceed 2.0. Pavement evenness deterioration results mostly from traffic loading and distress of pavement structure observed as fatigue cracks and rutting. Nevertheless, climatic distresses like frost heave (Sylvestre et al., 2017) and thermal cracking (Bae, Stoffels, Clyne, Worel, & Chehab, 2007) contribute to deterioration of evenness and a resultant increase in IRI as well. Differential settlement of embankment or subgrade may also influence the longitudinal roughness of pavement surface. The modelling and prediction of increase in roughness is therefore a complex problem and the factors that should be taken into account are not limited to effects of traffic loading. However, an increase in pavement roughness results in an increase in dynamic loads of vehicles and, consequently, in faster pavement structure deterioration.

Most of researchers reported linear dependence between IRI and DLC as it is visible in table 1. However as studies of (Jacob & Dolcemascolo, 1998) shows, the relationship is a power function with exponent < 1 due to non-linearity of the spring or damper parts. It should be emphasized that numerous researches based on simulations of road profiles and different approaches are used for this purpose, what can influence on the estimated values of DLC, which are given in table 1. The problem is wider described in the studies of (P. Múčka, 2017).

Table 1. Summary of relationships between Dynamic Load Coefficient DLC, vehicle speed and pavement roughness expressed by IRI

Study	Method: measurements or simulation (based on a model of vehicle or axle)	Value or range of speed [km/h]	Smoothness of pavement or range of IRI [m/km]	Range of DLC or model equation [-]
(Kazemi et al., 2018)(Woodrooffe, HF, &, & LePiane., 1986)	Measurements of five-axle truck with semi-trailer	40 – 80	0.88	0.04 – 0.08
			1.37	0.05 – 0.14
			1.52	0.05 – 0.16
			1.82	0.06 – 0.22
			3.17	0.07 – 0.27
(Bilodeau, Gagnon, & Doré, 2017)	2D half truck model simulation	100	0.683 – 7.612	$DLC_{100} = 0.0482\ IRI_{100} + 1$
(Park et al., 2014)	2D half truck model simulation	60	0.9	0.8 – 0.85
		60	2.7	1.4 – 1.5
(Chen, He, King, Chen, & Zhang, 2013; Peter Múčka, 2017b)	Measurements of three-axle semitrailer	60	6.21	0.079
		70	7.6	0.103
		80	8.88	0.177
(Elischer, Trevorrow, Callaway, & Blanksby, 2012; Peter Múčka, 2017b)	Measurements of three-axle semitrailers	80	1.85 – 5.44	$DLC = 0.068\ IRI + 0.021$ (mechanical, unladen) $DLC = 0.021\ IRI + 0.054$ (air, unladen) $DLC = 0.016\ IRI + 0.044$ (mechanical, laden) $DLC = 0.015\ IRI + 0.040$ (air, laden)
(Misaghi et al., 2010)	Simulation of Single axle (quarter car),	8 - 137	1.1 – 17.4	$DLC = 0.00085 \cdot IRI \cdot V$
	Simulation of tandem and tridem	8 - 137	1.1 – 17.4	$DLC = 0.00075 \cdot IRI \cdot V$
	Simulation of tandem walking beam axles	> 8 < 40	1.1 – 17.4	$DLC = 0.0027 \cdot V \cdot IRI$
		> 40 < 137	1.1 – 17.4	$DLC = 0.0004 \cdot V + 0.1129 \cdot IRI$
(Jacob & Dolcemascolo, 1998)	Measurements of two axle tractor	30	1.73	0.008 – 0.025
		80		0.035 – 0.038
(Moran & Sullivan, 1995)	Measurements	N/D	Smooth	0.289 – 0.596
(Sweatman, 1983)	Measurements of multiple axle loads	40	Smooth	0.02 – 0.04
		40	Rough	0.10 – 0.15
		80	Smooth	0.03 – 0.10
		80	Rough	0.15 – 0.40
(Hassan & McManus, 2001)	Simulation of five-axle tractor-semitrailer	100	1 – 5	$DLC = 0.0186 \cdot (IRI)^{1.026}$

N/D – no data available in the publication

Effect of vehicle dynamic loads on pavement response and deterioration

(Cebon, 1999) reported that dynamic forces are irrelevant to rutting damage, where gross vehicle weight is the dominant factor. Conversely, dynamic forces are important in fatigue damage, where relatively low levels of dynamic loads can lead to theoretical damage of up to 2.5 times the value of damage for static loads. The impact of dynamic forces may result in a 90% underprediction of fatigue damage at the end of the designed pavement life. For thicker flexible pavements, dynamic tyre loads have little impact on fatigue life.

In the study of (Rys, Judycki, & Jaskula, 2016b), the effect of vehicle dynamic loads on load equivalency factors was assessed. Analysis showed that load equivalency factor may increase up to 1.5 times when IRI increases to the value of 4.0 mm/m, resulting in a decrease in pavement life by 35%. (Khavassefat, Jelagin, & Birgisson, 2015, 2016) performed mechanistic analysis of pavement response under dynamic loads and reported that horizontal stress at the surface and the bottom of the asphalt layer can increase approximately by 50% for a flexible pavement with rougher profile (IRI = 2.3 m/km) in comparison to a smoother profile with IRI = 0.99 m/km. (Bilodeau et al., 2017) reported that the calculated pavement service life may be reduced by about 29% and 20% for bottom-up fatigue cracking and structural rutting failure criteria respectively, when dynamic loads are considered.

Determination of axle load spectra for pavement design

Currently axle load spectra for pavement design are determined on the basis of Weigh in Motion data, rarely on the basis of measurements delivered from static weight scales. Examples of application of axle load spectra in calculation of load equivalency factors were published by (Rys, Judycki, & Jaskula, 2016a; Turochy, Timm, & Tisdale, 2005) and (Atkinson, Merrill, & Thom, 2005). According to the Mechanistic-Empirical

Pavement Design Guide (NCHRP, 2004) and the report of (Atkinson et al., 2005) axle load spectra characterize traffic loads of pavement and are determined individually for single, tandem, tridem and quad axles, across separate vehicle classes and months. The following works include studies of implementing axle load spectra in M-EPDG calculations: (Haider & Harichandran, 2007; Tran & Hall, 2006; Turochy, Baker, & Timm, 2005; Wang, Donn, & Kamyar, 2007; Zofka, Urbaniak, Maliszewski, Bańskowski, & Sybilski, 2014). Most common axle load spectra for pavement design and analysis are expressed by a discrete percentage distribution in particular load intervals. On the basis of discrete distribution, load spectra can be modelled as cumulative distribution functions from regression models (Wang et al., 2007; Wu, 1996) or can be characterized by mixed distribution modelling (Haider, Harichandran, & Dwaikat, 2009; Macea, Márquez, & LLinás, 2015; Mohammadi & Shah, 1993; Timm, Tisdale, & Turochy, 2005). Dynamic loads of vehicles have been not considered in determination of axle load spectra yet. The main aim of this study is to fill in this gap in the knowledge.

Proposed approach

Determination of axle load spectra including dynamic loads of vehicles

WIM systems are calibrated using standard procedures that compare measurements obtained from WIM and from static scales. Dynamic effects of moving vehicles, beside other factors like pavement temperature or axle load sensor type (P. Burnos & Rys, 2017), causes inaccuracy of the WIM measurement. The role of calibration procedures and algorithms used in WIM systems is to ensure as high accuracy of data as it is possible . Thus axle load spectra obtained from WIM data represents distribution of static loads. Dynamic load distribution considered in the axle

load spectra aims to include and control the effect of deviations of axle loads from static magnitudes.

The discrete distribution of axle loads is characterized by percentage of axle passes falling into a set of axle load intervals Static Axle Load Spectrum (further abbreviated to SALS) is visible as column series in Figure 1 and the percentage of axle observations in particular load interval i is marked as s_i. The Dynamic Axle Loads Spectrum (further abbreviated to DALS) includes both SALS and distributions of dynamic loads coming from particular axle load intervals. In DALS the number of observations in a given axle load interval j is a sum of observations of dynamic loads being close to the static load Q_j (differing from the load Q_j so slightly that they fall into the range of the same load interval) as well as observations of dynamic loads resulting from all other intervals (coming from any other given SALS interval k, but, due to the distribution of its dynamic loads, falling within the range of the interval j). An example distribution of dynamic axle loads resulting from static loads Q_k is marked in Figure 1 as horizontal lines series. The formula (1) is used to calculate the percentage of dynamic loads d_j in the interval j coming from dynamic loads caused by axles with static loads Q_k.

$$d_j(Q_k) = s_k \frac{1}{\sigma(Q_k)\sqrt{2\pi}} \cdot exp\left(-\frac{(Q_k - Q_j)^2}{2\sigma(Q_k)^2}\right) = s_k \frac{1}{DLC\ Q_k\sqrt{2\pi}} \cdot exp\left(-\frac{(Q_k - Q_j)^2}{2\ DLC^{\,2} Q_k^2}\right) \quad (1)$$

where: $d_j(Q_k)$ – percentage of observations of dynamic loads Q_j caused by axles with static load Q_k, s_k – percentage of number of axles with static load Q_k determined from SALS, DLC – dynamic load coefficient, j, k – designations of load intervals.

In DALS the total percentage d_j of all axle loads falling in a given load interval j is calculated as a sum of dynamic loads coming from all the SALS intervals k(k from 1

to n, including k = j). The percentage of dynamic loads d_j is calculated according to the equation (2).

$$d_j = \sum_{k=1}^{n} d_j(Q_k) = \sum_{k=1}^{n} s_k \frac{1}{DLC\, Q_k \sqrt{2\pi}} \cdot exp\left(-\frac{(Q_k - Q_j)^2}{2DLC^2 {Q_k}^2}\right) \quad (2)$$

while:

$$\sum_{j=1}^{n} d_j(Q_k) = s_k \quad (3)$$

where all designations are the same as in equation (1).

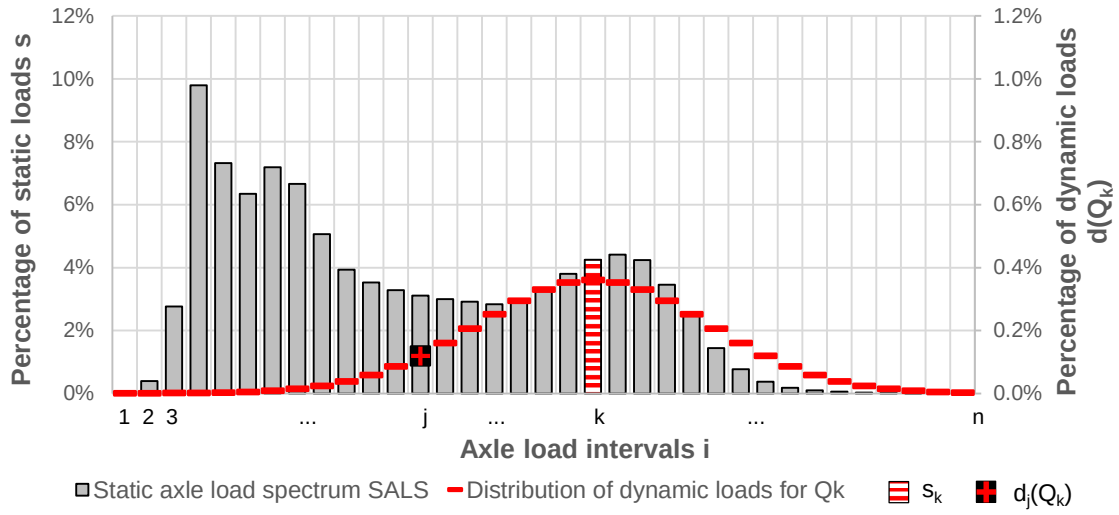

Figure 1. Example scheme of static load spectrum and distribution of dynamic loads obtained for mean load Q_k

It was assumed that each static load Q_i has a normal distribution of dynamic loads characterized by mean value lying in the middle of a given interval Q_i and standard deviation σ_i = DLC Q_i. It was assumed that DLC is constant for a given pavement roughness and vehicle speed over the full range of axle loads. Nevertheless, there is no limitation in the method to include variable values of DLC or introduce other distributions of dynamic loads than the Gaussian.

Sample calculations of dynamic axle load spectra

The sample calculations of dynamic axle load spectra were performed on the basis of data delivered from a Weigh in Motion station localized on the national road DK 7 near Cracow in Poland. The GPS coordinates of the WIM station for traffic moving south are N 50.3998674, E 20.0951576 and for traffic moving north: N 50.371812, E 20.0454665. The measurements covered a continuous period from January 2012 to December 2015, except several days of technical service. In total more than 18.3 million passes across all types of vehicles were recorded (including cars, vans etc.), out of which almost 1.9 million records of trucks were used in the analysis.

To ensure low measurement error, the WIM station is calibrated at least once a year and meets the requirements of the B+ standard according to the European COST 323 WIM specification. Nevertheless the raw WIM data were verified using a series of filters based on vehicle parameters (e.g. axle loads, total length, axle configurations etc.). The filters were set in accordance with the WIM Data Analyst's Manual (Quinley, 2010) and NCHRP Report 538 (NCHRP, 2005) as well as vehicle technical parameters review. The filtering process was focused on identifying and removing invalid records from the database. Vehicle records were removed when:

- Vehicle gross weight was lower than 35 kN;
- Axles loads were lower than 5 kN or greater than 200 kN;
- Vehicle length was lower than 3 m or greater than 20 m;
- Gaps between neighbouring axles were lower than 0.5 m;
- Vehicle speed was lower than 5 km/h or higher than 180 km/h;
- Record was uncompleted or flagged with the WIM system error.

In further step of data verification steering axle load spectra of selected vehicle group was analysed according to methodology developed in studies (Rys, 2019). For this part of data verification only group of 2-axle truck with 3-axle semi-trailer and with the gross weight limited to a range of 16 Mg to 20 Mg was selected. Spectra of steering axle load have a normal distribution and they were determined for particular month in analysed measurement period. Means of steering axle load spectra ranged from 52 kN to 58 kN and standard deviations of this spectra ranged from 3 kN to 5 kN. According to studies (Rys, 2019) such ranges of means and standard deviations of steering axle load spectra ensure satisfactory accuracy of WIM data and exclude possibilities of bias or too high random error in data set.

According to the M-EPDG, axle load spectra are determined in four groups: single, tandem, tridem and quad, separately for each month and each of nine vehicle classes (classified according to the FHWA standard). In order to make the analysis clearer, in this paper the axle load spectra were determined in three groups, excluding quad axles due to their very low frequency of appearance (below 0.1%). Axle load spectra are presented in Figure 2 for single, tandem and tridem axles respectively, without distinction between separate vehicle classes or different months. In Figure 2 axle load spectra determined directly from WIM data are marked as static loads (SALS). DALS presented in Figure 2 were calculated according to equation (2) on the basis of initial axle load spectra SALS. DALS are presented at different values of DLC. If DLC = 0, the dynamic loads do not occur and DALS and SALS coincide with each other. In real conditions, pavement surface is uneven and dynamic loads increase with the increase of IRI value as well as with an increase in vehicle speed. Consequently, the DLC parameter also increases.

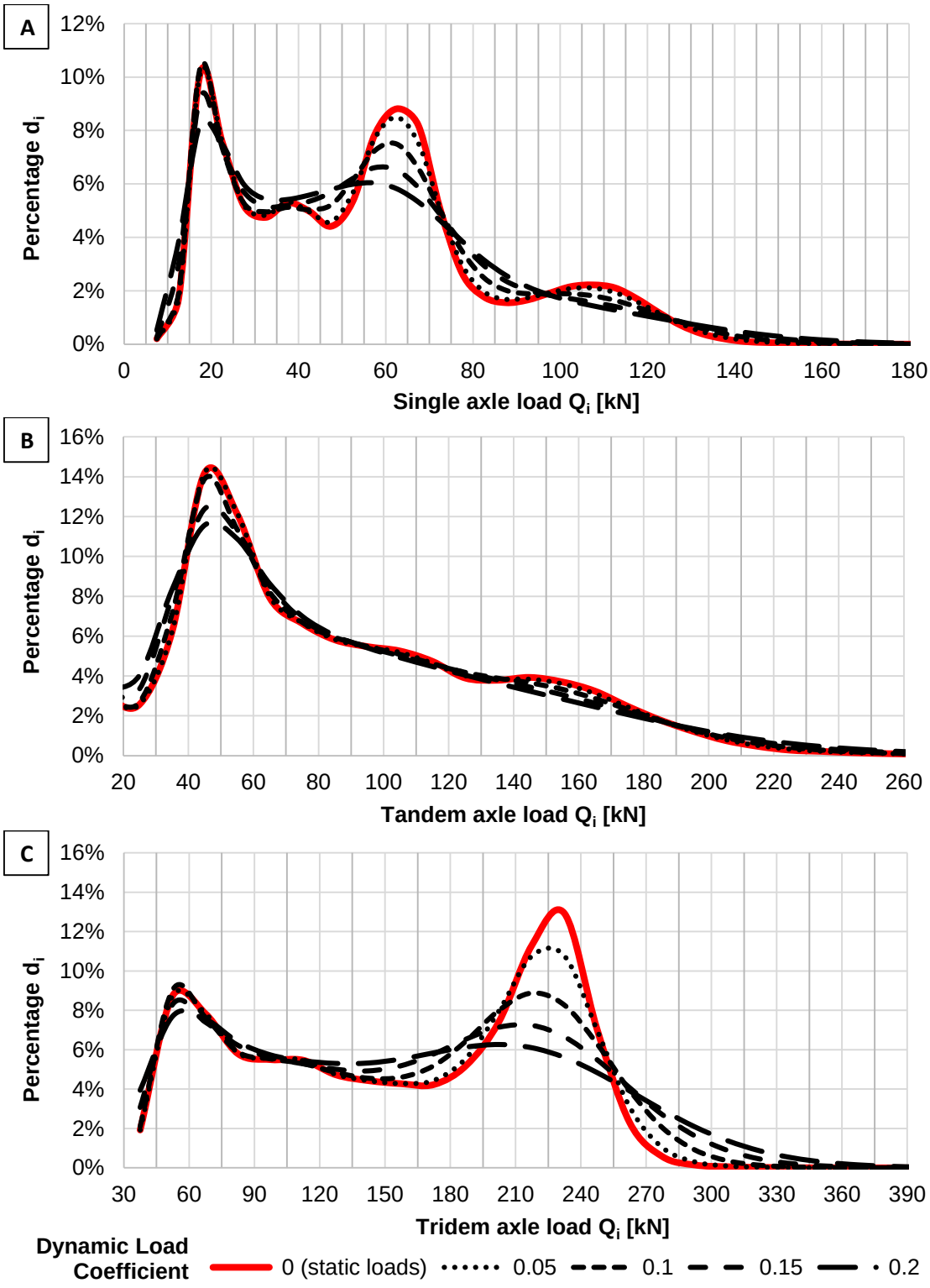

Figure 2. Spectra of axle loads obtained for WIM data (static loads) and with consideration of dynamic loads and various levels of DLC A) single axles B) tandem axles C) tridem axles

It is visible in Figure 2 that an increase in the DLC parameter causes an increase in percentage of the heaviest axle loads with a simultaneous decrease in percentage of lighter loads. Taking into account the fact that with an increase in axle load the detrimental effect of axle on the pavement structure increases with the approximate exponent of 4, higher dynamic loads significantly contribute to faster pavement distress. Because for most engineers the DLC parameter is not equally obvious as vehicle speed and IRI, in further analysis DALS were calculated for various IRI and vehicle speed values. The approximate values of IRI and vehicle speed corresponding to the given level of DLC were calculated on the basis of model determined by (Misaghi et al., 2010) given in Table 1. At a constant vehicle speed v = 60 km/h, values of DLC ranging from 0.05 to 0.2 correspond to values of IRI from 1.0 mm/m (smooth pavement) to 4.0 mm/m (degraded pavement). Calculations were performed for vehicle speeds from 30 km/h to 90 km/h and IRI from 1.0 mm/m to 4.0 mm/m. The maximum DLC considered in the analysis equals 0.306.

Analysis of the effect of dynamic loads on performance of flexible pavement

Pavement structure input data

For the analysis three flexible pavement structures were assumed according to the Polish Catalogue of Typical Flexible and Semi-Rigid Pavements (General Directorate for National Roads and Highways, 2014). Each structure consists of asphalt layers laid on a 20 cm base made of crushed stone as well as lower unbound layers. The total thickness of asphalt layers varies for particular structures and equals:

(1) KR1 – 9 cm, representative of thin structures,

(2) KR4 - 20 cm representative of structures for moderate traffic,

(3) KR7 - 30 cm representative of thick structures.

More detailed information about particular layer thicknesses and material designations is given in Figure 3.

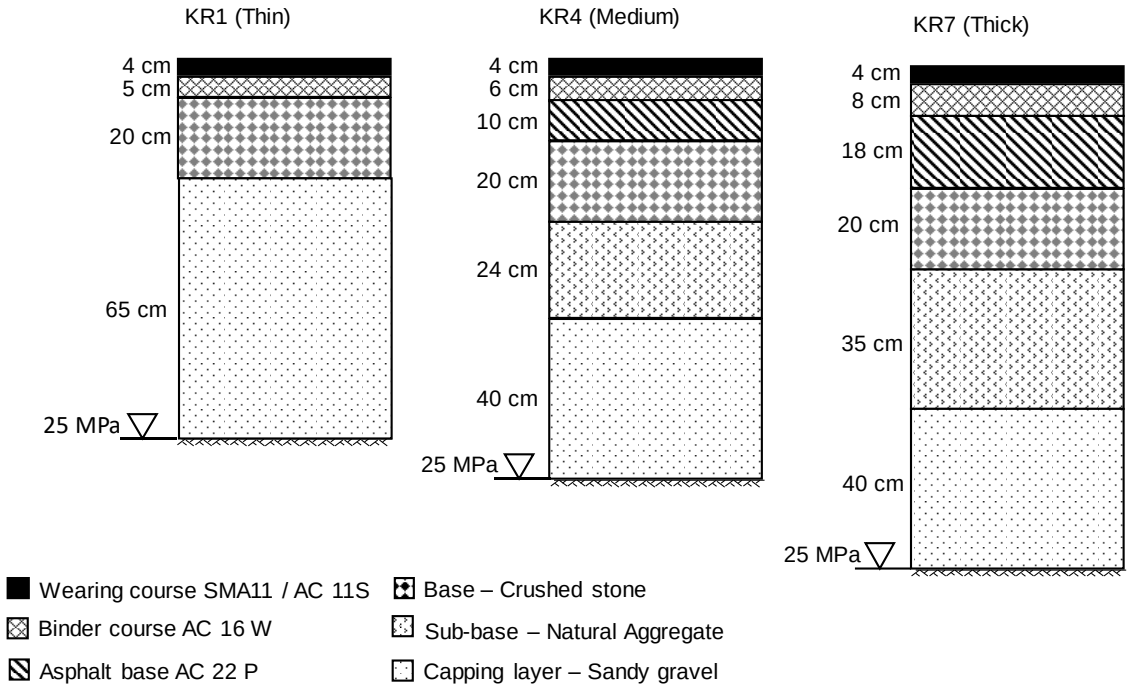

Figure 3. Scheme of flexible pavement structures assumed in the analysis

All of the asphalt mixtures meet requirements given in the Polish specification for asphalt mixtures WT-2 2014, which are in accordance with European standardisation. The volumetric properties of asphalt layers correspond to average design values assumed for the Polish catalogue of typical flexible and semi-rigid structures and they are summarized in Table 2. The master curves of asphalt mixtures are given in Figure 4 and were assumed after previous research works performed at the Gdansk University of Technology. More details regarding the properties of asphalt mixtures assumed for pavement design in Polish conditions are included in the following publications: (Judycki et al., 2017, 2014; Pszczola, Jaczewski, Rys, Jaskula, & Szydlowski, 2018; Stienss, Mejlun, & Judycki, 2016).

Table 2. Volumetric properties of asphalt layers

Layer	Mixture designation	Asphalt binder (UE standard and PG designation)	Air voids (%)	Effective binder content (%)
Wearing course	SMA 11 for KR4 and KR7	45/80-55 (PG 76-22)	3.0	16.0
	AC 11S for KR1	50/70 (PG 64-22)	2.5	14.0
Binder course	AC 16W for KR4 and KR7	35/50 (PG 70-22)	6.0	10.5
	AC 16W for KR1	50/70 (PG 64-22)	6.0	11.0
Asphalt base	AC 22P for KR4 and KR7	35/50 (PG 70-22)	7.0	10.0

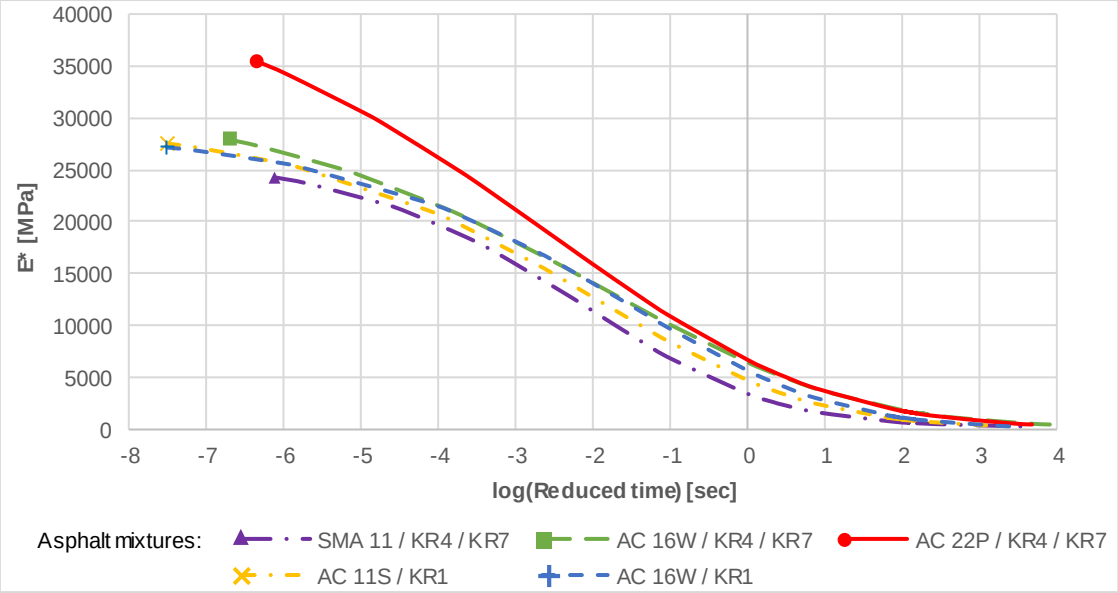

Figure 4. Master curves of asphalt mixes used in the analysis

The basic properties of unbound layers and subgrade are presented in Table 3. They were also assumed to represent common values used in pavement design in Poland.

Table 3. Properties of unbound layers and subgrade

Layer	Material	CBR (%)	Elastic modulus [MPa]	Liquid limit (%)	Plasticity index (%)
Base	Crushed stone 0/31.5	-	400	-	-
Sub-base	Natural aggregate 0/63	60	250	-	-
Capping layer	Sandy gravel	20	120	-	-
Subgrade	Clay	2	27	26	15

Traffic and climatic input data

The main variable in traffic input data are the axle load spectra, which are modified in dependence of DLC (see Figure 2). The remaining traffic input data for a given pavement structure are constant and they are summarized in Table 4. The values

of initial AADT were assumed in dependence of pavement structure to result in similar terminal IRI > 3.0 mm/m after 30 years of service for static axle load spectra. The AADT is assumed to consist exclusively of trucks, whose average number of axles and average axle spacing were based on WIM data analysis.

Table 4. Traffic input data for the M-EPDG pavement analysis

Traffic parameter	Assumed values
Initial two-way Annual Average Daily Traffic AADT	150 (KR1 thin structure) 1600 (KR4 medium structure) 6000 (KR7 thick structure)
Compound growth factor	3%
Percent of trucks in design direction	50%
Design lane width	3.5 m
Axle per Truck	1.98 (single) 0.18 (tandem) 0.34 (tridem)
Average axle spacing	1.4 m (tandem) 1.3 m (tridem)
Tyre pressure	850 kPa
Volume Monthly Adjustment Factors	Default MAF

The environmental data required to perform analysis in the M-EPDG were obtained from the Institute of Meteorology and Water Management (IMGW). The data include air temperature, wind speed, precipitation, humidity and sunshine, recorded on hourly basis in the period from 1 January 1994 to 31 December 2017. The study performed by (Pszczola, 2018; Pszczoła, Rys, & Jaskula, 2017) includes a more detailed analysis of environmental data obtained from Polish weather stations along with determination of zones of Performance Grade of asphalt binders and equivalency temperature for pavement design. For analysis in this paper, a station localized near the city of Lodz (N 51.756, E 19.444) was assumed to represent the moderate environmental conditions for Poland. The basic climatic statistics for the weather station Lodz are as follows:

- mean annual air temperature: 8.73°C,
- maximum/minimum air temperature: 37.5°C/-30.1°C,
- mean annual precipitation: 603.25 mm,
- freezing index: 258.86°C-days,

- average annual number of freeze/thaw cycles: 61.4,
- number of wet days: 165.2.

Calculation of pavement distress

The software AASHTOware ME Design v.2.3.1 was used to perform calculations of pavement deterioration in accordance with the M-EPDG approach. The distress models of asphalt pavements are described in details in (ARA Inc., 2004). The national US calibration factors were assumed for each distress model. The same 90% reliability level was assumed for each considered structure. Pavements distresses were calculated month by month up to 30 year of service. The terminal distress of pavement after 20 and 30 years of service calculated with the application of static load spectra is summarized in Table 5.

Table 5. Summary of predicted pavement distress after 20 and 30 years of service and application of static load spectra at reliability 90% for 3 types of pavement structures KR1 (thin), KR4 (medium) and KR7 (thick)

Distress type	20 years of service			30 years of service		
	KR1	KR4	KR7	KR1	KR4	KR7
AC Bottom-Up Fatigue Cracking [%]	2.08	2.75	2.00	7.13	9.16	2.48
AC Top-Down Fatigue Cracking [m/km]	57.58	50.13	49.11	63.70	51.21	49.49
AC Thermal cracking [m/km]	4.98	47.46	51.31	4.99	74.74	82.85
Permanent deformation of AC layers [mm]	1.85	8.97	12.88	2.32	11.65	16.77
Total permanent deformation [mm]	14.53	22.17	23.85	15.80	25.60	28.32
Terminal IRI [mm/m]	2.6	2.8	2.6	3.01	3.33	3.14

Table 5 presents all types of distress considered in the M-EPDG for flexible pavements. However, not all of them were considered in further analysis. AC thermal cracking does not result from traffic loading and was excluded. AC top-down cracking model provided surprisingly low values and a very slight increase in cracked area after 30 years of service, which indicates that local calibration is necessary. In consequence, top-down cracking was excluded from further analysis as well. The local calibration of M-

EPDG models has not been performed for Polish conditions yet. Nevertheless results delivered from globally calibrated M-EPDG models corresponds to field observations of LTPP sections and results are reasonable and realistic in the case of bottom-up cracking and permanent deformation. Finally, those two types of pavement distress were considered.

To evaluate the sensitivity of pavement performance to dynamic loads, a series of calculations was performed. Axle load distributions were assumed for analysis in dependence of the dynamic load coefficient DLC, which resulted from vehicle speed and IRI. Vehicle speed was considered in two places: 1) as a value input directly into M-EPDG procedure and 2) as a variable put into model developed by Misaghi et al. (2010) (see table 1) which both with IRI deliver DLC and has an impact on dynamic axle load spectra. IRI was considered as an initial value in M-EPDG procedure.

An example series of calculations for structure KR4, vehicle speed 60 km/h and various IRI values from 1 mm/m to 4 mm/m is presented in Figure 5. I should be noticed that in real conditions high values of initial IRI (above 2 mm/m) can appear rarely and locally. In most cases they are caused by some unexpected failures (eg. uncontrolled subsidence of the embankment). Figure 5 shows the calculated distress accumulation over 30 years of service when dynamic loads are included in the axle load spectra and, for comparison, when the axle load spectra represent only static loads.

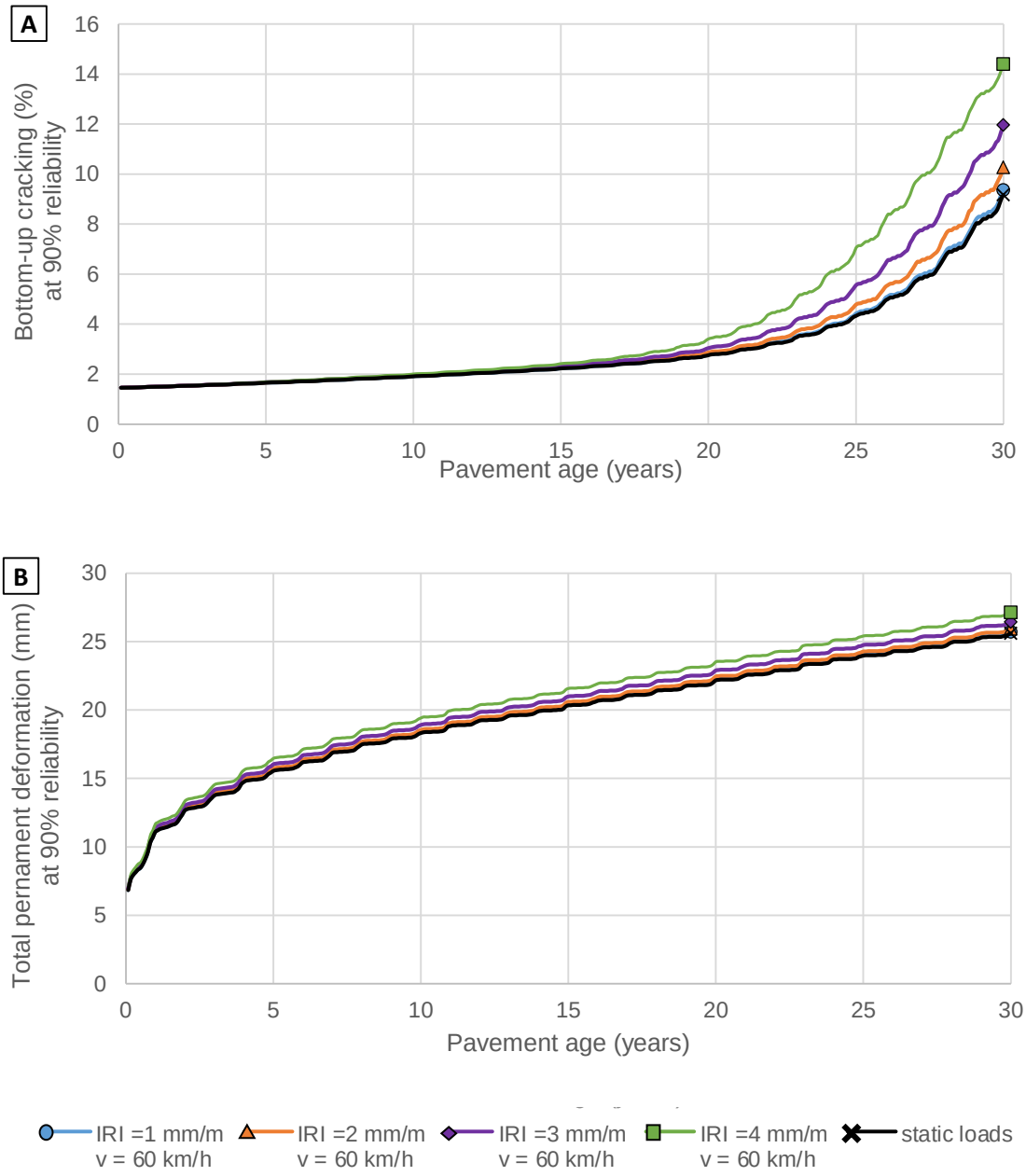

Figure 5. Results of calculation of pavement distress in accordance with the M-EPDG: A) bottom-up cracking B) total permanent deformation

In the example shown in Figure 5 it is visible that an increase in IRI (deterioration of pavement smoothness) results in higher terminal bottom-up cracked lane area and slightly faster progression of pavement distress. After 30 years of service, the structure may show cracked area higher by 67% and total rut deeper by 8%. In the case of old, degraded pavement, the dynamic loads contribute to much faster development of bottom-up cracks and less intensive increase in total rut depth. The effect of dynamic

loads on bottom-up cracks is almost invisible for the first 15 years of pavement service, but after that time higher dynamic loads, resulting from higher values of IRI cause faster increase in bottom-up cracks. For example, when static loads are considered, after 20 years of service the calculated percentage of bottom-up cracked area equals FC = 2.75%. If dynamic loads are considered, pavement is rough and its IRI = 4.0 mm/m, the same percentage of lane area is cracked after 17 years of service, 3 years earlier than in the case of static loads. It seems that dynamic loads has insignificant effect on total permanent deformation. However if the increments in total rut depth in particular years are compared to differences obtained for various IRI, the effect of IRI is visible. For example increase in IRI from 1 mm/m to 4 mm/m causes similar effect as 4 years of pavement service.

Impact of dynamic loads on decrease in service period length

Shortening of service period (ending with the appearance of distress at a given level) implies the adverse effect of dynamic loads of vehicles. To investigate susceptibility of pavement performance to dynamic loads, the following ratio was introduced:

$$SPR = \frac{SP_{f,s} - SP_{f,d}}{SP_{f,s}} \quad (4)$$

SPR – service period ratio [%],

$SP_{f,d}$ – service period to occurrence of a given distress level *f* obtained for dynamic axle load spectra DALS [years],

$SP_{f,s}$ – service period to occurrence of a given distress level *f* obtained for static axle load spectra SALS [years].

There are two possible ways to assume service period for equation 4:

1. to assume threshold for pavement distresses and then to determine time to achieve this level of distresses. For example structure KR4 and percentage of

assumed cracked lane area FC=5% the service period equals SPf,s = 26.1 years (for SALS).

2. to assume service period as a typical design period. In Poland and also in many other countries minimum service period for flexible pavements equals 20 years (SPf,s = 20 years). To obtain SPR, calculations of distress are first performed for a set service period $SP_{f,s}$ using SALS, and, treating the resulting distress f as threshold failure value for dynamic analysis, followed by DALS calculations of service period to failure $SP_{f,d}$.

According to the M-EPDG analysis, the process of pavement deterioration, visible in Figure 5, is not linear and intensifies with time. Therefore, value of service period ratio SPR depends on service period $SP_{f,s}$. Different approaches (assumed service periods ore failure threshold values) can lead to slight differences in calculated SPR values but the overall tendencies remain the same.

It was assumed that the designed service period of pavement structure for SALS equals 20 years. For $SP_{f,s}$= 20 years, the level of distress f (AC bottom-up cracks or total permanent deformation) occurring on pavement were determined. They are presented in Table 5. The service periods $SP_{f,d}$ to appearance of the same distress levels f for DALS were determined and SPR ratios were calculated according to equation (4). SPR ratios were calculated separately for the two chosen distress types (bottom-up cracking and total pavement deformation) and are presented in Figures 6 and 7.

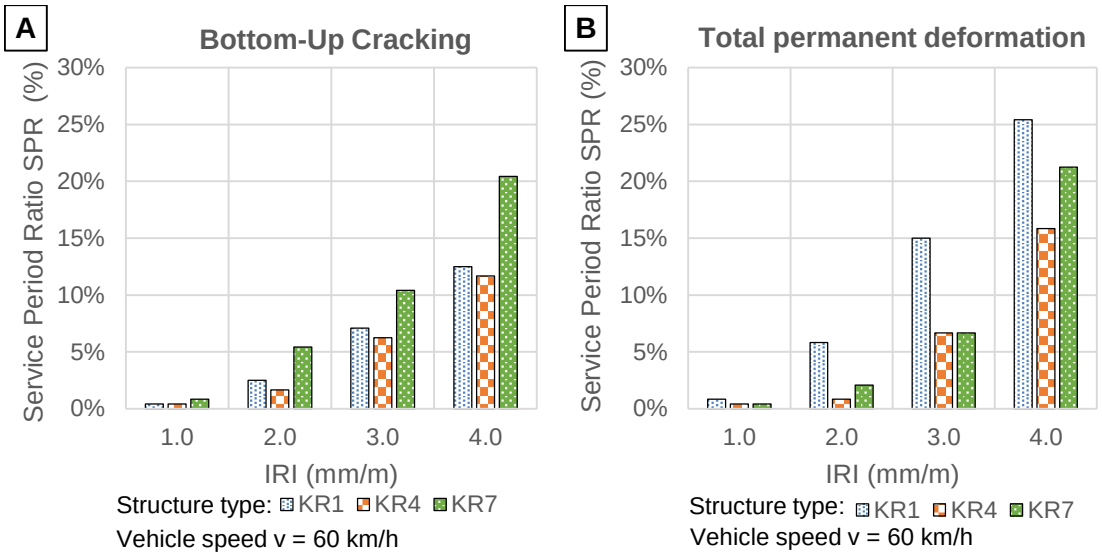

Figure 6. Service period ratio in dependence of structure thickness and surface roughness obtained for: A) bottom-up cracking B) total permanent deformation

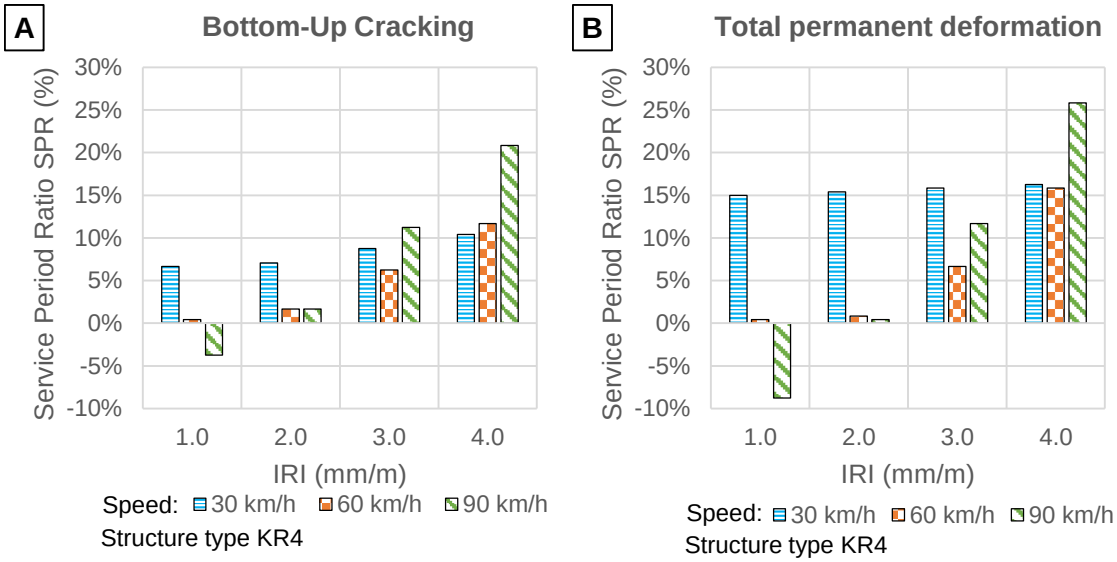

Figure 7. Service period ratio in dependence of vehicle speed and surface roughness obtained for the medium structure KR4 and distress types: A) bottom-up cracking B) total permanent deformation

On the basis of Figures 6 and 7 it can be stated that for smooth pavements with IRI close to 1.0 mm/m the dynamic loads of vehicles have minor effect on pavement performance. Nevertheless, with the deterioration of pavement smoothness, dynamic loads accelerate pavement distress. As shown in Figure 6, faster pavement distress due

to dynamic loads is noticeable both for thin, medium and thick pavements, while thin pavements are the most susceptible to dynamic loads and will exhibit permanent deformation up to 25% faster for rough surface with IRI = 4.0 mm/m. In the case of thick structures, deterioration of pavement evenness contributes more visibly to an increase in bottom-up cracking than in the case of thinner ones.

,A decrease in vehicle speed associates with increase in loading time and causes a decrease in stiffness moduli of asphalt mixtures (see Figure 4). In consequence tensile horizontal strains at the bottom of asphalt layers and vertical compressive strain calculated in the middle of thickness of each layer calculated at critical points of pavement structure increase while axle load remains constant. The M-EPDG fatigue cracking model (ARA Inc., 2004) relates the amount of estimated fatigue cracks with the horizontal tensile strain at the bottom of asphalt layers. Analogously in the permanent deformation models accumulated plastic strain is proportional to the vertical resilient strain. Therefore decrease in vehicle speed contribute to faster fatigue damage and increase in plastic deformations accumulated after each load repetition due to asphalt material properties and pavement response. Contrarily with a decrease in vehicle speed the dynamic load coefficient DLC also decreases what contribute to general lighter loading of pavement. In consequence of that both accumulation of fatigue damage and accumulation of plastic deformation are less intense according to M-EPDG models. It has a positive effect and contributes to lengthening of the service period.

Both the contrary effects related with vehicle speed are included in the calculation of the SPR ratio and the results are visible in Figure 7. On one hand, a decrease in vehicle speed from 60 km/h to 30 km/h causes a decrease in service period by 15% due to faster accumulation of permanent deformation (see Figure 7B for IRI=1.0 mm/m). On the other hand, deterioration of pavement evenness (see Figure 7B for IRI>1.0 mm/m) and

the resulting dynamic loads do not significantly contribute to faster pavement distress at low speeds (30 km/h) and SPR remains on the level of 15% (in comparison to 60 km/h). In the case of bottom-up cracking increase of IRI from 1.0 mm/m to 4.0 mm/m at constant low value of speed 30 km/h slightly impacts on decrease in service period.

The opposite effect is observed at high vehicle speeds (90 km/h). Higher vehicle speed means shorter loading time and increase in stiffness modulus of asphalt layers. Consequently at constant axle load pavements response with lower values of strains at critical points therefore accumulation of fatigue damage and permanent deformation is less intense than at lower speeds. This positive effect is visible in Figure 7 for pavement surface (IRI=1.0 mm/m). Service period increases up to 9% when vehicle speed increase from 60 km/h to 90 km/h. Nevertheless with simultaneous increase in vehicle speed and deterioration of pavement evenness (increase in IRI) dynamic loads intensify significantly. At the speed of 90 km/h, the effect of uneven surface with IRI = 4.0 mm/m on the increase in rut depth is higher than the effect of a decrease in vehicle speed to 30 km/h and service period shortens by 25% in relation to vehicle speed 60 km/h. If increase of IRI from 1 mm/m to 4 mm/m at constant speed 90 km/h is considered, the effect is much more visible and service period shortens up to 34%.

According to analysis, dynamic vehicle loads have minor effect on pavement performance when vehicle speed is low (30 km/h or less) even if pavement is rough (IRI is close to 4 mm/m). When pavement is properly maintained and IRI is close to 1.0 mm/m the dynamic effect of moving vehicles can be neglected. Dynamic vehicle loads contribute to faster pavement deterioration at speed equal to or higher than 60 km/h and IRI above 2 mm/m. It leads to the statement that the proper pavement evenness maintenance is crucial especially on high speed motorways.

Summary

Dynamic axle load spectra include both static axle load spectra and distributions of dynamic loads coming from particular axle load intervals. An increase in dynamic loads, expressed by an increase in dynamic load coefficient DLC, causes an increase in percentage of the heaviest axle loads with a simultaneous decrease in percentage of the lighter ones. Taking into account the fact that with an increase in axle load the detrimental effect of axle on pavement structure increases with the approximate exponent of 4, higher dynamic loads significantly contribute to faster pavement distress.

More detailed analyses of deterioration process of three sample flexible pavements (thin, medium and thick) were performed according to the Mechanistic-Empirical Pavement Design Guide using AASHTOware software. When dynamic loads were considered and pavement roughness index IRI equalled 4.0 mm/m, distress calculations of the medium pavement structure after 30 years of service resulted cracked area higher by 67% and total rut deeper by 8% than in the case of static load spectra.. The detrimental effects of dynamic axle loads increase rapidly with pavement evenness deterioration, resulting in up to 25% faster development of pavement distresses for IRI = 4.0 mm/m and vehicle speed 60 km/h. Dynamic loads have a minor effect on pavement performance when pavement is smooth and IRI is close to 1.0 mm/m.

The analysis proved that thinner pavement structures are more sensitive to dynamic loads. The investigation of impact of vehicle speed on vehicle dynamic loads and pavement performance showed that at a low vehicle speed dynamic loads have minor effect and decrease in vehicle speed from 60 km/h to 30 km/h causes a decrease in service period by 15% due to faster accumulation of permanent deformation regardless its roughness.. For vehicle speeds higher than 90 km/h dynamic loads significantly contribute to pavement distress and adverse dynamic effects are not compensated by the higher values of stiffness modulus of asphalt mixtures. Analysis

showed that increase in IRI to 4.0 mm/m and increase in vehicle speed from 60 km/h to 90 km/h causes decrease in service period by 25%.

Pavement roughness is typically considered as an effect of pavement deterioration and terminal IRI is used as a rate of pavement performance. As this analysis shows, due to dynamic effects, pavement roughness causes an increase in dynamic loads and contributes to faster pavement distress. Pavement roughness, beside material properties, traffic loads and climatic conditions, should be considered in analyses of pavement performance. Results of the analysis also emphasize the significance of proper pavement evenness maintenance, especially on high speed motorways.

Literature

Abdelaziz, N., Abd El-Hakim, R. T., El-Badawy, S. M., & Afify, H. A. (2018). International Roughness Index prediction model for flexible pavements. *International Journal of Pavement Engineering*, *8436*, 1–12. https://doi.org/10.1080/10298436.2018.1441414

Amarendra Kumar, S., & Ashoke Kumar, S. (2013). Development of a model for estimating International Roughness Index from pavement distresses. *International Journal of Pavement Engineering*, *14*(8), 715–724. https://doi.org/10.1080/10298436.2012.703322

ARA Inc. (2004). *Guide for Mechanistic-Empirical Design of New and Rehabilitated Pavement Structures. Part 3. Chapter 3. Design of New and Reconstructed Flexible Pavements.* Washington: Transportation Research Board.

Atkinson, V. M., Merrill, D., & Thom, N. (2005). *Pavement wear factors, TRL*

Published Project Report PPR 066.

Bae, A., Stoffels, S., Clyne, T., Worel, B., & Chehab, G. (2007). Direct effects of thermal cracks on pavement roughness. *Asphalt Paving Technology: Association of Asphalt Paving Technologists-Proceedings of the Technical Sessions*, *76*, 59–83.

Bilodeau, J. P., Gagnon, L., & Doré, G. (2017). Assessment of the relationship between the international roughness index and dynamic loading of heavy vehicles. *International Journal of Pavement Engineering*, *18*(8), 693–701. https://doi.org/10.1080/10298436.2015.1121780

Buhari, R., Md Rohani, M., & Abdullah, M. E. (2013). Dynamic Load Coefficient of Tyre Forces from Truck Axles. *Applied Mechanics and Materials*, *408*, 1900–1911. https://doi.org/10.4028/www.scient

Burnos, P., & Rys, D. (2017). The effect of flexible pavement mechanics on the accuracy of axle load sensors in vehicle weigh-in-motion systems. *Sensors (Switzerland)*, *17*(9). https://doi.org/10.3390/s17092053

Burnos, Piotr, Gajda, J., Piwowar, P., Sroka, R., Stencel, M., & Zeglen, T. (2007). Accurate weighing of moving vehicles. *Metrology and Measurement Systems*, *14*(4), 507–516.

Can, C., Williams, R. C., Marasinghe, M. G., Ashlock, J. C., Smadi, O., Schram, S., & Buss, A. (2016). Assessment of Composite Pavement Performance by Survival Analysis. *Journal of Transportation Engineering*, *142*(2), 548–556. https://doi.org/10.1061/(ASCE)TE.1943-5436

Cebon, D. (1999). *Handbook of Vehicle-Road Interaction*. Swets & Zeitlinger.

Chen, Y., He, J., King, M., Chen, W., & Zhang, W. (2013). Effect of driving conditions and suspension parameters on dynamic load-sharing of longitudinal-connected air suspensions. *Science China Technological Sciences*, *56*(3), 666–676. https://doi.org/10.1007/s11431-012-5091-3

Cole, D. J., and D. C. (1989). Simulation and Measurement of Dynamic Tyre Forces. *Cambridge University Press*.

Cole, D. J., & Cebon, D. (1992). Validation of an Articulated Vehicle Simulation. *Vehicle System Dynamics*, *21*(1), 197–223. https://doi.org/10.1080/00423119208969009

Davis, L. (2010). Dynamic Wheel Loads From Heavy Vehicles. *Queensland Roads Technical-Journal*, (6), 11.

Davis, L., & Bunker, J. (2011). Altering heavy vehicle air suspension dynamic forces by modifying air lines. *International Journal of Heavy Vehicle Systems*, *18*(1). https://doi.org/10.1504/IJHVS.2011.037957

De Beer, M., & Fisher, C. (2013). Stress-In-Motion (SIM) system for capturing tri-axial tyre-road interaction in the contact patch. *Measurement: Journal of the International Measurement Confederation*, *46*(7), 2155–2173. https://doi.org/10.1016/j.measurement.2013.03.012

Elischer, M., Trevorrow, N., Callaway, L., & Blanksby, C. (2012). *Measurement and Analysis of Dynamic Wheel Loads*. Sydney, Australia.

Gajda, J., Burnos, P., & Sroka, R. (2018). Accuracy Assessment of Weigh-in-Motion Systems for Vehicle's Direct Enforcement. *IEEE Intelligent Transportation*

Systems Magazine, *10*(1), 88–94. https://doi.org/10.1109/MITS.2017.2776111

General Directorate for National Roads and Highways, (GDDKiA). (2014). *Catalog of Typical Flexible and Semi-Rigid Pavements*. Gdansk. Retrieved from https://www.gddkia.gov.pl/userfiles/articles/z/zarzadzenia-generalnego-dyrektor_13901/zarzadzenie 31 zalacznik.pdf

Gillespie, T. D., Karamihas, S. M., Sayers, M., Nasim, M. A., Hansen, W., Ehsan, N., & Cebon, D. (1992). *Effects of heavy vehicles characteristic on pavement response and performance*.

Haider, S. W., & Harichandran, R. S. (2007). Relating Axle Load Spectra to Truck Gross Vehicle Weights and Volumes. *Journal of Transportation Engineering*, *133*(12), 696–705. https://doi.org/10.1061/(ASCE)0733-947X(2007)133:12(696)

Haider, S. W., Harichandran, R. S., & Dwaikat, M. B. (2009). Closed-Form Solutions for Bimodal Axle Load Spectra and Relative Pavement Damage Estimation. *Journal of Transportation Engineering*, *135*(12), 974–983. https://doi.org/10.1061/(ASCE)TE.1943-5436.0000077

Hassan, R., & McManus, K. (2001). Estimating dynamic load of pavements from surface profile properties. *Road And Transport Research*, *10*(3).

Imine, H., Delanne, Y., & M'Sirdi, N. K. (2006). Road profile input estimation in vehicle dynamics simulation. *Vehicle System Dynamics*, *44*(4), 285–303. https://doi.org/10.1080/00423110500333840

Jacob, B., & Dolcemascolo, V. (1998). Dynamic Interaction Between Instrumented Vehicles and Pavements. In *International Symposium on Heavy Vehicle Weights*

and Dimensions (pp. 142–160). Queensland, Australia.

Judycki, J., Jaskula, P., Pszczoła, M., Ryś, D., Jaczewski, M., Alenowicz, J., & Dołżycki, B. (2014). *Analysis and Design of Flexible and Semi-Rigid Pavements*. Warsaw, Poland.

Judycki, J., Jaskuła, P., Pszczoła, M., Ryś, D., Jaczewski, M., Alenowicz, J., … Stienss, M. (2017). New polish catalogue of typical flexible and semi-rigid pavements. In *MATEC Web of Conferences* (Vol. 122). https://doi.org/10.1051/matecconf/201712204002

Kazemi, S. F., Sebaaly, P. E., Siddharthan, R. V., Hajj, E. Y., Hand, A. J. T., & Ahsanuzzaman, M. (2018). Dynamic pavement response coefficient to estimate the impact of variation in dynamic vehicle load. *Bearing Capacity of Roads, Railways and Airfields - Proceedings of the 10th International Conference on the Bearing Capacity of Roads, Railways and Airfields, BCRRA 2017*, 433–441. https://doi.org/10.1201/9781315100333-63

Khavassefat, P., Jelagin, D., & Birgisson, B. (2015). Dynamic response of flexible pavements at vehicle–road interaction. *Road Materials and Pavement Design*, *16*(2), 256–276. https://doi.org/10.1080/14680629.2014.990402

Khavassefat, P., Jelagin, D., & Birgisson, B. (2016). The non-stationary response of flexible pavements to moving loads. *International Journal of Pavement Engineering*, *17*(5), 458–470. https://doi.org/10.1080/10298436.2014.993394

Macea, L. F., Márquez, L., & LLinás, H. (2015). Improvement of Axle Load Spectra Characterization by a Mixture of Three Distributions. *Journal of Transportation Engineering*, *141*(12), 04015030. https://doi.org/10.1061/(ASCE)TE.1943-

5436.0000801

Misaghi, S., Nazarian, S., & C. J. Carrasco. (2010). Impact of Truck Suspension and Road Roughness on Loads Exerted to Pavements. *Fhwa-Rd-07-1008-02*, *79968*(November).

Mohammadi, B. J., & Shah, N. (1993). Statistical evaluation o f t r u c k overloads, *118*(5), 651–665.

Moran, T., & Sullivan, M. (1995). Replication of Heavy Truck Dynamic Wheel Loads Using a Road Simulator. *Road Transport Technology*, *4*, 309–316. Retrieved from http://road-transport-technology.org/Proceedings/4 - ISHVWD/Replication Of Heavy Truck Dynamic Wheel Loads Using A Road Simulator - Moran .pdf

Múčka, P. (2017). Simulated Road Profiles According to ISO 8608 in Vibration Analysis. *Journal of Testing and Evaluation*, *46*(1), 20160265. https://doi.org/10.1520/jte20160265

Múčka, Peter. (2017a). International Roughness Index specifications around the world. *Road Materials and Pavement Design*, *18*(4), 929–965. https://doi.org/10.1080/14680629.2016.1197144

Múčka, Peter. (2017b). Road roughness limit values based on measured vehicle vibration. *Journal of Infrastructure Systems*, *23*(2), 1–13. https://doi.org/10.1061/(ASCE)IS.1943-555X.0000325

NCHRP. (2004). Mechanistic Empirical Pavement Design Guide. Retrieved August 3, 2018, from http://www.trb.org/mepdg/home.htm

NCHRP. (2005). *Traffic Data Collection, Analysis, and Forecasting for Mechanistic*

Pavement Design. Washington. https://doi.org/10.17226/13781

Park, D. W., Papagiannakis, A. T., & Kim, I. T. (2014). Analysis of dynamic vehicle loads using vehicle pavement interaction model. *KSCE Journal of Civil Engineering*, *18*(7), 2085–2092. https://doi.org/10.1007/s12205-014-0602-3

Perera, R. W., Byrum, C., & Kohn, S. D. (1998). *Investigation of Development of Pavement Roughness*. *FHWA-RD-97-147*. https://doi.org/10.1017/CBO9781107415324.004

Pszczola, M. (2018). Equivalent temperature for design of asphalt pavements in Poland. In *Scientific Conference of the Committee for Civil Engineering of the Polish Academy of Sciences and the Science Committee of the Polish Association of Civil Engineering, Krynica Zdroj* (pp. 1–6).

Pszczola, M., Jaczewski, M., Rys, D., Jaskula, P., & Szydlowski, C. (2018). Evaluation of asphalt mixture low-temperature performance in bending beam creep test. *Materials*, *11*(1). https://doi.org/10.3390/ma11010100

Pszczoła, M., Rys, D., & Jaskula, P. (2017). Analysis of climatic zones in Poland with regard to asphalt performance grading. *Roads and Bridges - Drogi i Mosty*, *16*(4), 245–264. https://doi.org/10.7409/rabdim.017.016

Quinley, R. (2010). *WIM Data Analyst ' s Manual*. *FHWA Report IF-10-018*.

Rys, D. (2019). Investigation of Weigh-in-Motion Measurement Accuracy on the Basis of Steering Axle Load Spectra. *Sensors*, *19(15)*(3272), 20–22. https://doi.org/10.3390/s19153272

Rys, D., Judycki, J., & Jaskula, P. (2016a). Analysis of effect of overloaded vehicles on

fatigue life of flexible pavements based on weigh in motion (WIM) data. *International Journal of Pavement Engineering*, *17*(8). https://doi.org/10.1080/10298436.2015.1019493

Rys, D., Judycki, J., & Jaskula, P. (2016b). Determination of Vehicles Load Equivalency Factors for Polish Catalogue of Typical Flexible and Semi-rigid Pavement Structures. In *Transportation Research Procedia* (Vol. 14). https://doi.org/10.1016/j.trpro.2016.05.272

Shi, X. M., & Cai, C. S. (2009). Simulation of Dynamic Effects of Vehicles on Pavement Using a 3D Interaction Model. *Journal of Transportation Engineering*, *135*(10), 736–744. https://doi.org/10.1061/(ASCE)TE.1943-5436.0000045

Stienss, M., Mejlun, L., & Judycki, J. (2016). Influence of selected WMA additives on viscoelastic behaviour of asphalt mixes and pavements, *8436*(June). https://doi.org/10.1080/10298436.2016.1199882

Sun, L. (2013). An overview of a unified theory of dynamics of vehicle-pavement interaction under moving and stochastic load. *Journal of Modern Transportation*, *21*(3), 135–162. https://doi.org/10.1007/s40534-013-0017-8

Sweatman, P. F. (1983). *A study of dynamic wheel forces in axle group suspensions of heavy vehicles*. *Australian Road Research Board, Research Report SR27*.

Sylvestre, O., Bilodeau, J. P., & Doré, G. (2017). Effect of frost heave on long-term roughness deterioration of flexible pavement structures. *International Journal of Pavement Engineering*, *8436*, 1–10. https://doi.org/10.1080/10298436.2017.1326598

Timm, D. H., Tisdale, S. M., & Turochy, R. E. (2005). Axle Load Spectra Characterization by Mixed Distribution Modeling. *Journal of Transportation Engineering*, *131*(2), 83–88. https://doi.org/10.1061/(ASCE)0733-947X(2005)131:2(83)

Tran, N. H., & Hall, K. D. (2006). Development and Influence of Statewide Axle Load Spectra on Flexible Pavement Performance. *Transportation Research Board*, *6660*(479).

Turochy, R. E., Baker, S. M., & Timm, D. H. (2005). Spatial and Temporal Variations in Axle Load Spectra and Impacts on Pavement Design. *Journal of Transportation Engineering*, *131*(10), 802–808. https://doi.org/10.1061/(ASCE)0733-947X(2005)131:10(802)

Turochy, R. E., Timm, D. H., & Tisdale, S. M. (2005). Truck Equivalency Factors, Load Spectra Modeling and Effects on PAvement Design.

Wang, Y., Donn, H., & Kamyar, M. (2007). Axle Load Distribution Characterization for Mechanistic Pavement Design. *Journal of Transportation Engineering*, *133*(8). https://doi.org/10.1061/(ASCE)0733-947X(2007)133:8(469)

Woodrooffe, HF, J., & P. A. L., & LePiane., K. R. (1986). Effects of Suspension Variations on the Dynamic Wheel Loads of a Heavy Articulated Highway Vehicle.

Wu, S.-S. (1996). Procedure to Estimate Loading From Weigh-in-Motion Data. *Transportation Research Record*, *1536*(1), 19–24. https://doi.org/10.3141/1536-03

Ziari, H., Sobhani, J., Ayoubinejad, J., & Hartmann, T. (2015). Prediction of IRI in short and long terms for flexible pavements: ANN and GMDH methods.

International Journal of Pavement Engineering, *17*(9), 776–788. https://doi.org/10.1080/10298436.2015.1019498

Zofka, A., Urbaniak, A., Maliszewski, M., Bańskowski, W., & Sybilski, D. (2014). Site specific traffic inputs for mechanistic-empirical pavement design guide in Poland. Transportation Research Board, Annual Meeting, Waszyngton, 2014. *Transportation Research Board 93rd Annual Meeting*.